High Energy Density Physics 18 (2016) 38–44

Contents lists available at ScienceDirect

High Energy Density Physics

journal homepage: www.elsevier.com/locate/hedp

A direct-drive exploding-pusher implosion as the first step in development of a monoenergetic charged-particle backlighting platform at the National Ignition Facility

M.J. Rosenberg [a,1,*], A.B. Zylstra [a,2], F.H. Séguin [a], H.G. Rinderknecht [a,3], J.A. Frenje [a], M. Gatu Johnson [a], H. Sio [a], C.J. Waugh [a], N. Sinenian [a], C.K. Li [a], R.D. Petrasso [a], S. LePape [b], T. Ma [b], A.J. Mackinnon [b], J.R. Rygg [b], P.A. Amendt [b], C. Bellei [b], L.R. Benedetti [b], L. Berzak Hopkins [b], R.M. Bionta [b], D.T. Casey [b], L. Divol [b], M.J. Edwards [b], S. Glenn [b], S.H. Glenzer [b], D.G. Hicks [b,4], J.R. Kimbrough [b], O.L. Landen [b], J.D. Lindl [b], A. MacPhee [b], J.M. McNaney [b], N.B. Meezan [b], J.D. Moody [b], M.J. Moran [b], H.-S. Park [b], J. Pino [b], B.A. Remington [b], H. Robey [b], M.D. Rosen [b], S.C. Wilks [b], R.A. Zacharias [b], P.W. McKenty [c], M. Hohenberger [c], P.B. Radha [c], D. Edgell [c], F.J. Marshall [c], J.A. Delettrez [c], V.Yu. Glebov [c], R. Betti [c], V.N. Goncharov [c], J.P. Knauer [c], T.C. Sangster [c], H.W. Herrmann [d], N.M. Hoffman [d], G.A. Kyrala [d], R.J. Leeper [d], R.E. Olson [d], J.D. Kilkenny [e], A. Nikroo [e]

[a] Plasma Science and Fusion Center, Massachusetts Institute of Technology, Cambridge, MA 02139, USA
[b] Lawrence Livermore National Laboratory, Livermore, CA 94550, USA
[c] Laboratory for Laser Energetics, University of Rochester, Rochester, NY 14623, USA
[d] Los Alamos National Laboratory, Los Alamos, NM 87545, USA
[e] General Atomics, San Diego, CA 92186, USA

ARTICLE INFO

Article history:
Received 7 August 2015
Received in revised form 23 October 2015
Accepted 6 January 2016
Available online 18 January 2016

Keywords:
Exploding-pusher implosions
Charged-particle backlighting
Nuclear diagnostics

ABSTRACT

A thin-glass-shell, D^3He-filled exploding-pusher inertial confinement fusion implosion at the National Ignition Facility (NIF) has been demonstrated as a proton source that serves as a promising first step toward development of a monoenergetic proton, alpha, and triton backlighting platform at the NIF. Among the key measurements, the D^3He-proton emission on this experiment (shot N121128) has been well-characterized spectrally, temporally, and in terms of emission isotropy, revealing a highly monoenergetic ($\Delta E/E \sim 4\%$) and isotropic source (~3% proton fluence variation and ~0.5% proton energy variation). On a similar shot (N130129, with D_2 fill), the DD-proton spectrum has been obtained as well, illustrating that monoenergetic protons of multiple energies may be utilized in a single experiment. These results, and experiments on OMEGA, point toward future steps in the development of a precision, monoenergetic proton, alpha, and triton source that can readily be implemented at the NIF for backlighting a broad range of high energy density physics (HEDP) experiments in which fields and flows are manifest, and also utilized for studies of stopping power in warm dense matter and in classical plasmas.

1. Introduction

The proton radiography technique [1,2] is a powerful tool in high-energy-density physics (HEDP) [3] research, providing precise images of electric and magnetic fields [4–10], as well as mass structures, in laser-generated plasma experiments. Two widely-used techniques for backlighter proton generation are the target normal sheath acceleration (TNSA) mechanism [11,12], in which a high-intensity laser irradiates a solid foil to accelerate protons, and monoenergetic charged-particle radiography [13,14], which uses fusion products

* Corresponding author. Plasma Science and Fusion Center, Massachusetts Institute of Technology, Cambridge, MA 02139, USA.
E-mail address: mros@lle.rochester.edu (M.J. Rosenberg).
[1] Present address: Laboratory for Laser Energetics, University of Rochester, Rochester, NY 14623, USA.
[2] Present address: Los Alamos National Laboratory, Los Alamos, NM 87545, USA.
[3] Present address: Lawrence Livermore National Laboratory, Livermore, CA 94550, USA.
[4] Present address: Swinburne University of Technology, Hawthorn, VIC 3122, Australia.

http://dx.doi.org/10.1016/j.hedp.2016.01.001
1574-1818/

from D^3He-filled "exploding pusher" inertial confinement fusion (ICF) implosions. The TNSA source offers excellent spatial (~10–20 μm) and temporal (~1–10 ps) resolution based on the properties of the backlighter laser, and generates a continuous spectrum of protons. The monoenergetic backlighting technique is particularly valuable in that it produces particles of a well-defined energy ($\Delta E/E$~2–5%) and superior uniformity of proton, alpha, and triton emission, enabling highly quantitative measurements. Additionally, the use of particles at different discrete energies allows for discrimination between electric and magnetic field effects and for studies of stopping power using the energy downshift of charged-particle spectra.

Monoenergetic charged-particle backlighting has been implemented and used extensively at the OMEGA laser facility [15]. This technique has provided quantitative information about fields produced in laser–foil interactions [16,17], magnetic reconnection [18,19], the Weibel instability [20], direct-drive ICF implosions [21–23], and indirect-drive ICF hohlraums [24,25]. In addition, this monoenergetic proton source has been used in experiments at OMEGA to study stopping power in warm dense matter (WDM) [26]. Though the monoenergetic charged-particle backlighting platform is well-established at OMEGA, it is only beginning to be implemented at the National Ignition Facility (NIF) [27], where a significantly greater laser energy, laser power, and spatial scale enables new regimes of HEDP experiments.

Presented here are results from a directly-driven D^3He-filled, thin-glass-shell exploding pusher implosion (shot N121128) [28], which serves as a promising first step toward the development of a baseline implosion design for monoenergetic charged-particle backlighting at the NIF. This experiment represents the first demonstration at the NIF of a monoenergetic proton source. Though this shot was conducted for diagnostic development and calibration, valuable ride-along data have been obtained, showing that this implosion serves as a useful guidepost for implementation of a monoenergetic charged-particle backlighting platform. The remainder of this paper is organized as follows: Section 2 describes the experimental setup and principal measurements that characterize this implosion and its utility as a monoenergetic proton source; and Section 3 discusses the next steps required in the implementation and usage of a monoenergetic charged-particle backlighting platform at the NIF.

2. Experimental setup and results

NIF exploding-pusher shot N121128 used a 1682-μm diameter, 2.2 g/cm^3 SiO_2 shell with a wall thickness of 4.3 μm, filled with 9.1 atm of D^3He gas (3.3 atm D_2 and 5.8 atm ^3He). The capsule was coated with 0.03 μm Al to reduce the leak rate of ^3He out of the capsule.[5] The capsule was irradiated by 192 NIF beams in the polar-direct-drive (PDD) configuration [29], delivering 43.4 kJ of laser energy in a 1.4-ns ramp pulse. The laser pulse and capsule properties are illustrated in Fig. 1 and summarized, along with the principal experimental measurements, in Table 1.

This implosion produced copious DD and D^3He fusion reactions:

$$D + D \rightarrow {}^3He(0.82\,MeV) + n(2.45\,MeV), \quad (1)$$

$$D + D \rightarrow T(1.01\,MeV) + p(3.02\,MeV), \text{and} \quad (2)$$

$$D + {}^3He \rightarrow \alpha(3.6\,MeV) + p(14.7\,MeV). \quad (3)$$

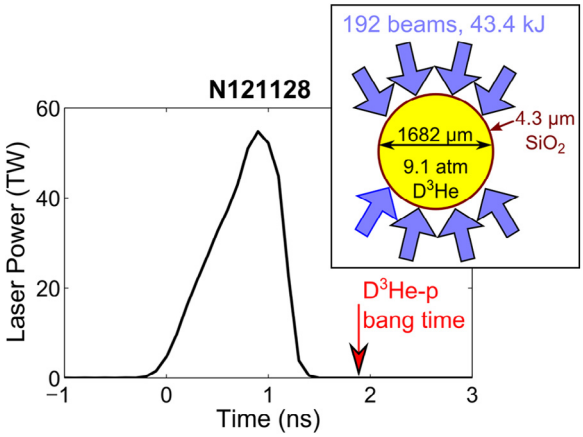

Fig. 1. (Color online) Experimental laser power history and capsule and laser parameters (inset) from NIF D^3He exploding pusher shot N121128. The time of peak D^3He-proton emission (bang time) at $t = 1.88$ ns, several hundred ps after the end of the laser pulse (~1.4 ns), is shown (see Fig. 2 for the raw proton bang time data).

The monoenergetic particle backlighting platform will be designed to utilize the D^3He protons and alphas (Equation 3) as well as the DD protons and tritons (Equation 2). Shot N121128 was diagnosed through measurements of DD-neutron (Equation 1) emission using the neutron time-of-flight (nTOF) suite [30] and primarily through measurements of D^3He-proton emission using wedge range filter (WRF) proton spectrometers [31–33] and the particle time-of-flight (pTOF) diagnostic [34]. As has been described in detail elsewhere [28], the nTOF-measured DD-neutron yield was 7.27×10^{10} (and based on the DD-n/DD-p branching ratio of ~0.98 at the measured DD-burn-averaged ion temperature of 7.1 keV, the DD-proton yield is expected to have been 7.4×10^{10}); the WRF-measured D^3He-proton yield was 2.09×10^{10}. Uncertainty in the DD-n yield measurement was ~ ±10%, while uncertainty in the D^3He-p yield measurement was around ±3% based on excellent spatial uniformity of the inferred proton yields. Yields of this magnitude are more than sufficient for charged-particle backlighting experiments at the NIF, where ideal particle fluences of ~10^5 cm^{-2} would be achieved at CR-39 [35,36] detectors positioned 50–200 cm from the experiments. Burn-averaged ion temperatures inferred from the Doppler width of the fusion-product spectra were inferred to be 7.1 ± 0.5 keV averaged over the DD-n reactions (measured by nTOFs) and 11.0 ± 2.0 keV averaged over the D^3He reactions (measured by WRFs) [28].[6] The difference between DD-burn-averaged and D^3He-burn-averaged ion temperatures is likely a consequence of the difference in temperature dependence of the fusion reactivity of reactions 1 and 3, with DD (D^3He) reactions weighted more strongly to the cooler (hotter) regions of the fuel. Thermal decoupling of ^3He and deuterium ions (with ^3He ions hotter due to stronger heating by the shock) [37] is another possible contributing factor. Using an independent measurement technique based on the ratio of DD and D^3He yields [38], the ion temperature was inferred to be 6.9 ± 1.0 keV, in reasonable agreement with the linewidth-inferred ion temperature. The total ρR was inferred from the downshift of the D^3He-p spectrum to be 9 ± 4 mg/cm^2. The time of peak D^3He-p emission (bang time) was measured by pTOF to be 1.88 ± 0.10 ns, several hundred ps after the end of the laser pulse [28]. The pTOF trace obtained on shot N121128, originally presented in Ref. [28], is shown in Fig. 2, illustrating a robust D^3He-p signal and minimal x-ray background.

[5] The fill was intended to be 3.3 atm D_2 and 6.7 atm ^3He for an equimolar mixture, but 0.9 atm of ^3He leaked out of the capsule in the 15 hours it was removed from the pressure vessel before it was shot, based on a leak rate half-life of 76 hours.

[6] These measurements assume that the width of the neutron and proton spectra are due entirely to thermal broadening and not to flows.

Table 1
Capsule and laser parameters and principal experimental measurements for NIF exploding pusher shot N121128, including: capsule outer diameter d; shell thickness Δr; total laser energy; approximate laser pulse duration; D_2 fill pressure; ^{3}He fill pressure; DD-n yield; D^3He-p yield; D^3He-p bang time (BT); approximate x-ray burn duration (based on similar shots); DD-burn-averaged ion temperature; D^3He-p burn-averaged ion temperature; DD/D^3He yield-ratio-inferred ion temperature; and total ρR.

Capsule		Laser		Gas pressure		Y_{DD-n}	Y_{D^3He-p}
d (μm)	Δr (μm)	Energy (kJ)	Duration (ns)	D_2 fill (atm.)	^{3}He fill (atm.)		
1682	4.3	43.4	~1.4	3.3	5.8	7.27×10^{10}	2.09×10^{10}
D^3He-p BT (ns)	X-Ray Duration (ns)	$T_{i,DD}$ (keV)	$T_{i,D3He}$ (keV)	$T_{i,ratio}$ (keV)	ρR_{total} (mg/cm^2)		
1.88 ± 0.10	0.20 ± 0.10	7.1 ± 0.5	11.0 ± 2.0	6.9 ± 1.0	9 ± 4		

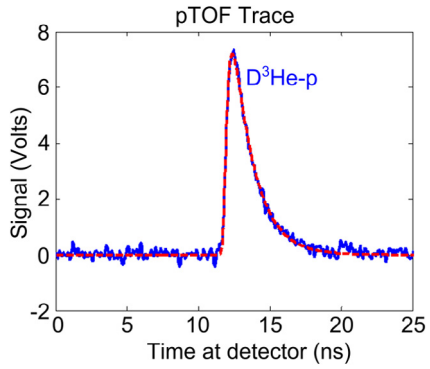

Fig. 2. (Color online) pTOF D^3He-p signal obtained on shot N121128 used to infer the proton bang time. A forward fit to these data shows that the D^3He-p bang time is 1.88 ns, as indicated in Fig. 1. These data were originally presented in Ref. [28]. Reproduced with permission from *Phys. Plasmas* **21**, 122712 (2014). Copyright 2014, AIP Publishing LLC.

X-ray measurements were also used to diagnose this implosion. The time of peak x-ray emission (x-ray bang time) was measured by the South Pole Bang Time (SPBT) diagnostic [39] and the hardened gated x-ray imager (hGXI) [40] to be 1.96 ± 0.07 ns and 2.04 ± 0.12 ns, respectively. On shots roughly comparable to N121128, N130129 and N110131 [28], hGXI or the gated x-ray detector (GXD) [41] measured the full-width at half maximum (FWHM) duration of x-ray emission to be ~0.20 ± 0.10 ns.[7] This measurement serves as a useful approximation (slight overestimate) of the duration of fusion emission,[8] and in future charged-particle backlighting experiments it will be important to directly obtain the fusion reaction history. In monoenergetic backlighting experiments on OMEGA, the D^3He-p burn duration was measured to be shorter, around 80–120 ps [13], using smaller capsules with a 420 μm diameter. Fig. 3 shows an hGXI x-ray self-emission image roughly 100 ps before bang time, originally presented in Ref. [28]; the image reveals a slightly oblate implosion with a second Legendre mode magnitude of P2/P0 = –0.13, and an overall radius of x-ray emission of 168 μm. The x-ray emission radius at bang time is extrapolated to be ~150 μm. The x-ray image gives an approximate size of the fuel region, though for monoenergetic particle backlighting it will be ideal to obtain an image of the fusion emission in order to directly characterize the particle source size. According to data obtained on previous experiments (discussed in Appendix A), there is a correlation between x-ray radius and fusion emission radius, with the fusion emission region of order 60% the size of the shell as inferred from x-ray emission. Though for stopping power experiments the fusion source size is not important, for proton radiography experiments the fusion source size sets the spatial resolution. A fusion emission radius of order 100 μm is a factor of ~4 larger than has been produced in proton radiography experiments on OMEGA, and a smaller source size is desired.

WRF-measured D^3He-proton spectra, two of seven obtained at different positions on shot N121128, are shown in Fig. 4. The proton spectra show a narrow, well-defined spectral line, with a mean energy of $\langle E \rangle = 14.45 \pm 0.06$ MeV (position 0-0-4) and $\langle E \rangle = 14.39 \pm 0.06$ MeV (position 90-78-1). The average over all seven positions is 14.42 MeV, with minimal variation, as discussed further below. The spectral width, inferred after accounting for the WRF instrumental broadening, is $\sigma = 0.25$ MeV, which corresponds to a D^3He-burn-averaged ion temperature of 11.0 keV as noted above. To quantify the monoenergetic character of this proton source, the energy spread ΔE is defined as the full-width at half-maximum (FWHM) of the D^3He-p spectrum ($\mathrm{FWHM} = 2\sqrt{2\ln 2}\sigma = 0.59$ MeV), and $\Delta E/\langle E \rangle = 0.59/14.42 = 4\%$. The monoenergetic character of the proton (or alpha or triton) spectra enables quantitative inferences of electric and magnetic field strengths from particle deflection in radiography experiments or precise measurements of energy loss in stopping power

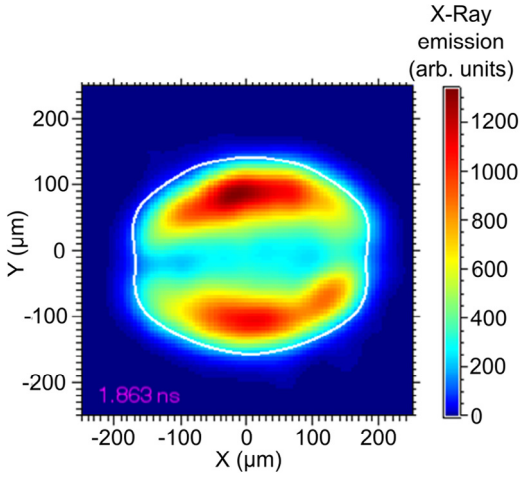

Fig. 3. (Color online) hGXI x-ray self-emission of the D^3He fuel region ~100 ps before bang time in shot N121128. The image, with the contour corresponding to 10% of the peak emission magnitude (white line) indicated, shows an average P0 =168 μm and a P2/P0 = –0.13 (13% oblate). The P0 at bang time is extrapolated to be ~150 μm. The image predominantly represents x-ray emission in the energy range of 8–10 keV. These data were originally presented in Ref. [28]. Reproduced with permission from *Phys. Plasmas* **21**, 122712 (2014). Copyright 2014, AIP Publishing LLC.

[7] SPBT gives x-ray bang time measurements, but not burn duration.
[8] 1D LILAC simulations show that for this class of implosion, the nuclear burn duration is slightly shorter than the x-ray burn duration, by around 10–50%. These simulations also indicate that the peak time of x-ray emission occurs of order 100 ps after the peak of D^3He emission, which was also observed on shot N121128.

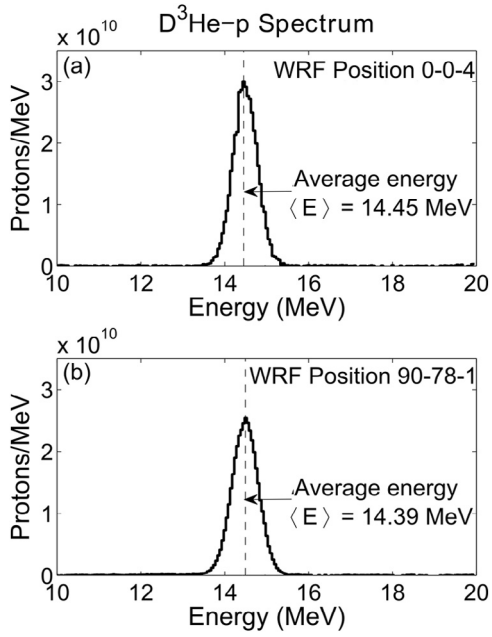

Fig. 4. Measured primary D^3He-proton spectrum from (a) the fourth WRF positioned near (0,0) and (b) the first WRF positioned near (90,78) on D^3He exploding-pusher shot N121128. As is discussed below and illustrated in Fig. 5, the proton spectra at seven positions around the NIF chamber were nearly identical in both mean proton energy and proton fluence.

experiments. For radiographic applications, the particle deflection angle due to electric (magnetic) fields is inversely proportional to the particle energy (velocity), so an energy (velocity) spread of 4% (2%) produces blurring of only a small percentage of the total deflection. This is especially valuable in diagnosing filamentary magnetic field structures as are expected to be produced in upcoming collisionless shock experiments at the NIF.

Though the DD-proton spectrum was not measured on this experiment, the modest energy downshift of the D^3He-p spectrum (from 14.7 MeV to 14.42 MeV) and DD-proton measurements obtained on a similar exploding pusher shot, D_2 filled N130129 [42], indicate that the ~3-MeV DD protons are readily usable as well for charged-particle backlighting experiments. The total areal density (ρR) inferred from the D^3He-proton energy downshift on shot N121128 is only 9 ± 4 mg/cm^2 [28], which suggests that the DD-proton energy on shot N121128 was likely around 2.3 ± 0.3 MeV. This is based on the relation between total ρR and the final charged-particle energy, $E_{final} = E_0 - \int_0^{\rho R_{total}} \frac{dE}{d\rho R}(E) d\rho R$, where E_0 is the birth energy and $\frac{dE}{d\rho R}$ is the energy-dependent stopping power. On shot N130129, with a slightly higher ρR, the mean DD-p energy was measured to be 2.0 MeV. For exploding-pusher implosions with a $\rho R < 20$ mg/cm^2, the DD protons escape the capsule, enhancing the utility of the implosion as a charged-particle source. A similar ρR permits the emission of D^3He alphas, while a $\rho R < 10$ mg/cm^2 is needed for DD tritons to escape the capsule (this does not account for filtering in the CR-39 detectors, so a ρR closer to 3–5 mg/cm^2 is likely needed to make use of the tritons).

Of particular importance for charged-particle backlighting is the spatial uniformity of both the emitted particle fluence and the emitted particle energy. Measurements of the uniformity of the D^3He-proton spectrum on shot N121128, based on seven WRFs (three near the equator (90,78) and four near the pole (0,0) relative to the NIF geometry) are shown in Table 2 and illustrated visually in Fig. 5. The spectra shown in Fig. 4 are taken from the Pole-4 and Equator-1 WRFs. These data show that the emitted D^3He-proton spectrum was

Table 2
Measured D^3He-proton yield and energy at seven different WRF positions (including their distance from the implosion) on shot N121128. The measurements on the equator were conducted at a fairly high fluence of protons (6×10^5 cm^{-2}) [43], and the capability to measure the D^3He-p energy using WRFs at significantly higher fluences has been developed [44]. The random energy uncertainty for each measurement is ~ ±60 keV, while the random yield uncertainty for each measurement is ~ ±5%. Excellent uniformity of the emitted proton fluence and energy show that this implosion has great utility as a monoenergetic charged-particle source. Even with many fewer beams, as required in a particle backlighting experiment, such isotropy in particle fluence and energy is likely achievable.

WRF position	Dist. (cm)	D^3He-p yield (10^{10})	D^3He-p energy (MeV)
Equator-1	50	2.01	14.39
Equator-3	50	2.17	14.34
Equator-4	50	2.14	14.40
Eq. Avg.		2.11	14.38
Pole-1	200	2.00	14.54
Pole-2	200	2.05	14.49
Pole-3	200	2.11	14.36
Pole-4	200	2.15	14.45
Pole Avg.		2.08	14.46
Overall Avg.		2.09	14.42

extremely uniform in both fluence and energy on shot N121128. The average fluence variation is <2% from pole to equator, with a 3% standard deviation overall. The high degree of fluence isotropy is enabled by designing the implosion so that nuclear bang time occurs several hundred ps after the end of the laser pulse. In proton backlighting experiments on OMEGA, a $26 \pm 10\%$ fluence variance was observed [14], though in those implosions, bang time occurred during the laser pulse and the protons may have been susceptible to electric and magnetic field effects around the backlighter capsule. In other OMEGA exploding pusher experiments where bang time was well after the end of the laser pulse, a much more uniform proton fluence was observed (variance $\lesssim 5\%$) [45,46], as on shot N121128. The mean D^3He-proton energy varies by only 80 keV between the polar and equatorial measurements, with an overall standard deviation of 65 keV. Thus, shot N121128 illustrates the potential for a highly uniform source of protons, as well as alphas and tritons, in both fluence and energy. An implosion with this degree of emission uniformity could simultaneously backlight multiple experiments along different lines of sight and also allow for the utilization of algorithms to directly infer path-integrated electric or magnetic field images from measured charged-particle fluence images [2]. Additionally, such excellent energy isotropy would enable studies of charged particle stopping power in laser-generated warm dense matter and classical plasmas, which rely on an assumption of particles of identical energy emitted along different lines of sight.

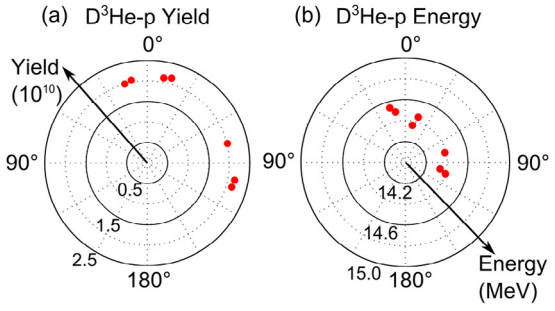

Fig. 5. (Color online) WRF-measured D^3He-p (a) yield and (b) energy as a function of polar angle on NIF for shot N121128. Excellent uniformity is observed, to ~ ±3% in inferred yield and ~ ±70 keV (~ ±0.5%) in energy, smaller than measurement uncertainties, as discussed in Table 2.

3. Implementation of the monoenergetic charged-particle backlighting platform at the NIF

Subsequent steps in the development of the monoenergetic charged-particle backlighting platform at NIF both utilize existing capabilities and require the implementation of new capabilities.

Many of the same instruments used to diagnose shot N121128, and several additional instruments, will be used to characterize a monoenergetic proton, alpha, and triton source at the NIF, based on the measurements described above. WRF proton spectrometers will be fielded at several different positions around the NIF chamber to measure the D^3He-p yield, mean proton energy, and linewidth. pTOF will measure the time of proton emission, necessary to ascertain the "sample time" of the charged particles at the subject. Given that minimal x-ray signal was observed on pTOF when filtered by 50 μm Ta and 100 μm Au on shot N121128 (Fig. 2), it is plausible that on a comparable implosion pTOF could be fielded with filtering thin enough to allow for detection of the DD protons as well, without being susceptible to x-rays. In addition to the absolute timing of particle emission, the duration of particle emission is important to measure directly in order to characterize the time-gating of the source. The duration of proton emission (likely ~100 ps) is too short to be measured using pTOF, and only x-ray burn duration measurements are currently available, using hGXI, GXD, and SPIDER [47]. To remedy this lack of a direct nuclear burn duration measurement, the development of a neutron temporal diagnostic (NTD) [48] capable of measuring burn histories on that time scale has been proposed for implementation at the NIF. As have been used previously, step range filter (SRF) proton spectrometers [42] will characterize the DD-p spectrum, and will be enhanced for alpha and triton energy measurements as well. Penumbral imaging of the DD and D^3He protons [49] will be used to measure the spatial extent of fusion emission, which determines the spatial resolution in charged-particle radiography experiments. For penumbral imaging measurements of the particle source size, existing GXD hardware would be used to place a 2 mm diameter aperture 10 cm from the backlighter implosion, with CR-39 detectors filtered by ~10 μm Ta (for DD-p or D^3He-α) and additionally by 1500 μm CR-39 and 200 μm Al (for D^3He-p) 130 cm from the backlighter. This technique is equivalent to that used in the Proton Core Imaging System (PCIS) on the OMEGA laser facility, which is discussed further in Appendix A.

In radiography experiments, the use of many charged particles on a single shot importantly allows for improved quantitative determination of path-integrated electric or magnetic field strengths and, especially, for discrimination between proton deflections due to electric fields or magnetic fields. In such experiments, CR-39 detectors will be affixed to the front of a diagnostic snout at a distance of 39 cm from the center of the NIF target chamber and filtered by ~40 μm Zr (for DD-p or D^3He-α) and an additional 1500 μm CR-39 and 200 μm Al (for D^3He-p). Measurements of charged-particle stopping power will use the existing WRF and SRF spectrometers at a distance of 50 cm from the subject, with spectra from the backlighter implosion diagnosed along one line-of-sight and energy-downshifted spectra after passing through the stopping-power target diagnosed along another line-of-sight.

In summary, direct-drive exploding-pusher shot N121128 demonstrates a promising starting point for development of a monoenergetic proton, alpha, and triton backlighting platform at the NIF, based on large, monoenergetic proton yields with a well-characterized time of proton emission and a high degree of isotropy of both proton fluence and energy. While all 192 beams were used to drive shot N121128, in a charged-particle backlighting experiment many fewer beams would be used, as some beams are needed to drive the primary target. A proposed design calls for 6 NIF "quads", with 24 beams in total, to drive the backlighter implosion at a similar laser energy (~40 kJ) to that used on shot N121128. Even under such conditions, excellent isotropy in particle fluence and energy is likely to be achieved in this exploding-pusher implosion, which have been shown in OMEGA experiments to be largely insensitive to illumination non-uniformities [50]. If greater drive uniformity on the backlighter capsule is required, it may also be possible to use an indirectly-driven exploding-pusher implosion, with a hole or a thin patch in the hohlraum wall in the direction of the subject plasma [51]. This would likely have to be driven by around half of the NIF beams in order to deliver ~0.6–1.0 MJ, as has been used in other indirectly-driven exploding pushers on NIF [52]. Excellent proton fluence isotropy has been observed through the hohlraum equator on indirectly-driven implosions at the NIF [53], and so indirectly-driven backlighter implosions would be expected to produce a similarly good fluence isotropy. A 24-beam backlighter direct-drive configuration would leave up to 168 beams available to drive targets for studies of electric and magnetic fields and flows in indirect-drive ignition-scale hohlraums, direct-drive implosions, collisionless shocks, and other ICF or HEDP experiments, as well as studies of stopping power in WDM and classical plasmas.

Most directly, the next steps in the development of the NIF monoenergetic charged-particle backlighting platform begin with experiments to characterize the charged-particle emission – including particle energies, spectral widths, and source profiles – for a 24-beam implosion source. These experiments, starting from the baseline conditions of shot N121128, seek to confirm that a 24-beam implosion using a similar laser energy and pulse shape produces similar particle yield, energy, and isotropy and that such an implosion is insensitive to drive asymmetries and beam selection. Initial tests are planned for the use of 24 NIF beams from the 45° and 50° drive cones (relative to the up-down axis of the NIF chamber) evenly split between the upper and lower hemispheres; later tests may use 16 or 32 beams from within the 45° degree cones in both hemispheres or a one-sided drive using the 45° and 50° degree cones from a single hemisphere for possible use in charged-particle radiography of half-hohlraums. A subsequent step will involve attempting to reduce the size of the charged-particle source using a smaller capsule, though this will require the removal of phase plates so as to produce sufficiently small laser beam profile on NIF, as has been done previously on OMEGA [13]. As discussed above, another crucial step is the installation and refinement of additional diagnostics, including penumbral imaging, lower-energy charged-particle spectrometry, nuclear burn history measurements, and the proton radiography diagnostics. The first experiments to utilize this charged-particle backlighting platform are scheduled to follow this development process.

The authors thank R. Frankel, E. Doeg, M. Cairel, M. Valadez, and M. McKernan for contributing to the processing of CR-39 data used in this work, as well as the NIF operations crew for their help in executing these experiments. This work was conducted in partial fulfillment of the first author's PhD thesis and supported in part by US DoE (Grant No. DE-NA0001857), FSC (No. 5-24431), LLE (No. 415935-G), and LLNL (No. B600100).

Appendix A. Nuclear burn imaging data in previous exploding pusher experiments on OMEGA

As discussed above, the size of the fusion emission region is a critical property of the monoenergetic charged-particle source. While spatially-resolved measurements of the fusion burn region have not yet been obtained directly on the NIF, previous exploding pusher experiments on OMEGA provide valuable insight into trends in the fusion source size.

A consistent correlation has been observed in some exploding-pusher experiments on OMEGA [46,54] between the measured fusion emission size and the radius of the shell as inferred from x-ray images. These measurements were obtained on implosions

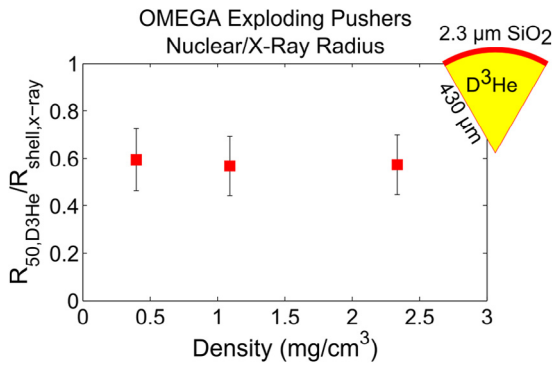

Fig. A6. (Color online) Measured ratio of the nuclear burn radius to x-ray-measured minimum shell radius as a function of initial D^3He gas density in exploding pusher experiments at OMEGA. These experiments used 2.3 μm thick, 860 μm diameter SiO_2 shells filled with equimolar D^3He gas and irradiated by 14.6 kJ laser energy (60 beams) in a 0.6 ns square pulse [46,54]. The nuclear burn radius is characterized as the radius containing 50% of the D^3He yield ($R_{50,D3He}$) [54], while the x-ray minimum shell radius ($R_{shell,x-ray}$) is approximately the radius of peak x-ray emission in the shell at stagnation. A near-constant ratio of $R_{50,D3He}/R_{shell,x-ray} \sim 0.58$ is observed.

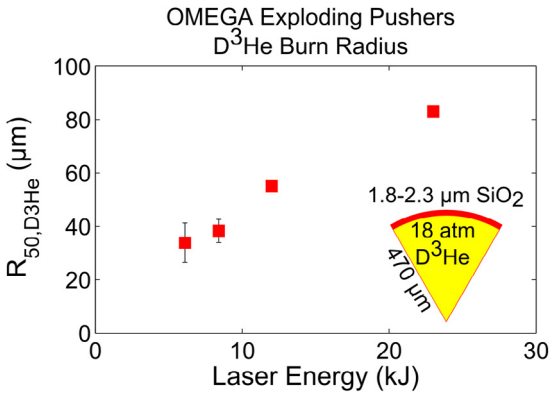

Fig. A7. (Color online) Measured D^3He burn radius as a function of laser energy in exploding pusher experiments at OMEGA. These experiments used 1.8–2.3 μm thick, 940 μm diameter SiO_2 shells filled with 18 atm (2.4 mg/cm^3) equimolar D^3He gas and irradiated by 60 OMEGA laser beams in a 0.6 ns square pulse [56]. The nuclear burn radius is characterized as the radius containing 50% of the D^3He yield. These data were originally presented in Ref. [56]. Reproduced with permission from *Phys. Plasmas* **13**, 082704 (2006). Copyright 2006, AIP Publishing LLC.

with a 2.3 μm thick, 860 μm diameter SiO_2 shell, containing different densities of equimolar D^3He gas and irradiated by 60 OMEGA laser beams that delivered 14.6 kJ in a 0.6 ns pulse. The D^3He-p emission radius was measured using the Proton Core Imaging System (PCIS) [49,54–56] and quantified as the radius containing 50% of the fusion reactions ($R_{50,D3He}$). The shell radius was characterized using x-ray framing cameras [57], based on the approximate radius of maximum local x-ray emission from the shell. The ratio of these two quantities, $R_{50,D3He}/R_{shell,x-ray}$ is shown as a function of the initial D^3He gas density in Fig. A6. Error bars account for the ~ ±10% uncertainty in the measured $R_{50,D3He}$ and the ~ ±20% uncertainty in the measured $R_{shell,x-ray}$. A near-constant ratio of $R_{50,D3He}/R_{shell,x-ray} = 0.58 \pm 0.01$ is observed at three different gas densities between 0.4 and 2.3 mg/cm^3. This correlation between the nuclear emission radius and the x-ray-inferred shell radius may hold true at the NIF scale as well, in which case the x-ray radius can be used to provide information about the fusion source size.

Additionally, a different set of prior exploding pusher experiments on OMEGA have demonstrated a trend of increasing burn radius with increasing laser energy [56]. These experiments used 1.8–2.3 μm, 940 μm diameter SiO_2 shells filled with 18 atm (2.4 mg/cm^3) equimolar D^3He gas and imploded by 60 OMEGA laser beams in a 1-ns square pulse at a variety of total laser energies. As described above, the D^3He fusion emission was measured using PCIS. The D^3He-p emission size (again characterized as the radius containing 50% of the reactions, $R_{50,D3He}$) is shown as a function of the incident laser energy in Fig. A7. The measurements show a monotonic and nearly linear trend of increasing fusion emission radius with laser energy. Though this parameter sweep represents only one set of exploding pusher conditions, the observed trend suggests that for purposes of proton radiography where having a small source size is critical, a lower laser energy may be preferable. These results ought to be considered when designing and optimizing a charged-particle backlighter at the NIF.

References

[1] A.J. Mackinnon, P.K. Patel, R.P. Town, M.J. Edwards, T. Phillips, S.C. Lerner, et al., Proton radiography as an electromagnetic field and density perturbation diagnostic (invited), Rev. Sci. Instrum. 75 (10) (2004) 3531–3536.

[2] N.L. Kugland, D.D. Ryutov, C. Plechaty, J.S. Ross, H.-S. Park, Invited article: relation between electric and magnetic field structures and their proton-beam images, Rev. Sci. Instrum. 83 (2012) 101301.

[3] R.C. Davidson, Frontiers in High Energy Density Physics, National Academies Press, Washington, DC, 2003.

[4] P.M. Nilson, L. Willingale, M.C. Kaluza, C. Kamperidis, S. Minardi, M.S. Wei, et al., Magnetic reconnection and plasma dynamics in two-beam laser-solid interactions, Phys. Rev. Lett. 97 (2006) 255001.

[5] C.A. Cecchetti, M. Borghesi, J. Fuchs, G. Schurtz, S. Kar, A. Macchi, et al., Magnetic field measurements in laser-produced plasmas via proton deflectometry, Phys. Plasmas 16 (2009) 043102.

[6] M. Borghesi, G. Sarri, C.A. Cecchetti, I. Kourakis, D. Hoarty, R.M. Stevenson, et al., Progress in proton radiography for diagnosis of ICF-relevant plasmas, Laser Part. Beams 28 (2010) 277–284.

[7] L. Willingale, P.M. Nilson, M.C. Kaluza, A.E. Dangor, R.G. Evans, P. Fernandes, et al., Proton deflectometry of a magnetic reconnection geometry, Phys. Plasmas 17 (2010) 043104.

[8] S.L. Pape, P. Patel, S. Chen, R. Town, D. Hey, A. Mackinnon, Proton radiography of magnetic fields in a laser-produced plasma, High Energy Dens. Phys. 6 (2010) 365–367.

[9] L. Gao, P.M. Nilson, I.V. Igumenshchev, S.X. Hu, J.R. Davies, C. Stoeckl, et al., Magnetic field generation by the Rayleigh-Taylor instability in laser-driven planar plastic targets, Phys. Rev. Lett. 109 (2012) 115001.

[10] G. Fiksel, W. Fox, A. Bhattacharjee, D.H. Barnak, P.-Y. Chang, K. Germaschewski, et al., Magnetic reconnection between colliding magnetized laser-produced plasma plumes, Phys. Rev. Lett. 113 (2014) 105003, doi:10.1103/PhysRevLett.113.105003.

[11] R.A. Snavely, M.H. Key, S.P. Hatchett, T.E. Cowan, M. Roth, T.W. Phillips, et al., Intense high-energy proton beams from petawatt-laser irradiation of solids, Phys. Rev. Lett. 85 (14) (2000) 2945–2948.

[12] A.B. Zylstra, C.K. Li, H.G. Rinderknecht, F.H. Séguin, R.D. Petrasso, C. Stoeckl, et al., Using high-intensity laser-generated energetic protons to radiograph directly driven implosions, Rev. Sci. Instrum. 83 (2013) 013511.

[13] C.K. Li, F.H. Séguin, J.A. Frenje, J.R. Rygg, R.D. Petrasso, R.P.J. Town, et al., Monoenergetic proton backlighter for measuring *E* and *B* fields and for radiographing implosions and high-energy density plasmas (invited), Rev. Sci. Instrum. 77 (2006) 10E725.

[14] M.J.-E. Manuel, A.B. Zylstra, H.G. Rinderknecht, D.T. Casey, M.J. Rosenberg, N. Sinenian, et al., Source characterization and modeling development for monoenergetic-proton radiography experiments on OMEGA, Rev. Sci. Instrum. 83 (2012) 063506.

[15] T.R. Boehly, D.L. Brown, R.S. Craxton, R.L. Keck, J.P. Knauer, J.H. Kelly, et al., Initial performance results of the omega laser system, Opt. Commun. 133 (1997) 495–506.

[16] C.K. Li, F.H. Séguin, J.A. Frenje, J.R. Rygg, R.D. Petrasso, R.P.J. Town, et al., Measuring *E* and *B* fields in laser-produced plasmas with monoenergetic proton radiography, Phys. Rev. Lett. 97 (2006) 135003.

[17] M.J.-E. Manuel, C.K. Li, F.H. Séguin, J. Frenje, D.T. Casey, R.D. Petrasso, et al., First measurements of Rayleigh-Taylor-induced magnetic fields in laser-produced plasmas, Phys. Rev. Lett. 108 (2012) 255006.

[18] C.K. Li, F.H. Séguin, J.A. Frenje, J.R. Rygg, R.D. Petrasso, R.P.J. Town, et al., Observation of megagauss-field topology changes due to magnetic reconnection in laser-produced plasmas, Phys. Rev. Lett. 99 (2007) 055001.

[19] M.J. Rosenberg, C.K. Li, W. Fox, I. Igumenshchev, F.H. Séguin, R.P.J. Town, et al., A laboratory study of asymmetric magnetic reconnection in strongly driven plasmas, Nat. Commun. 6 (2015) 6190.

[20] C.M. Huntington, F. Fiuza, J.S. Ross, A.B. Zylstra, R.P. Drake, D.H. Froula, et al., Observation of magnetic field generation via the Weibel instability in interpenetrating plasma flows, Nat. Phys. 11 (2015) 173–176.

[21] C.K. Li, F.H. Séguin, J.R. Rygg, J.A. Frenje, M. Manuel, R.D. Petrasso, et al., Monoenergetic-proton-radiography measurements of implosion dynamics in direct-drive inertial-confinement fusion, Phys. Rev. Lett. 100 (2008) 225001.
[22] J.R. Rygg, F.H. Séguin, C.K. Li, J.A. Frenje, M.J.-E. Manuel, R.D. Petrasso, et al., Proton radiography of inertial fusion implosions, Science 319 (2008) 1223–1225.
[23] F.H. Séguin, C.K. Li, M.J.-E. Manuel, H.G. Rinderknecht, N. Sinenian, J.A. Frenje, et al., Time evolution of filamentation and self-generated fields in the coronae of directly driven inertial-confinement fusion capsules, Phys. Plasmas 19 (2012) 012701.
[24] C.K. Li, F.H. Séguin, J.A. Frenje, M. Rosenberg, R.D. Petrasso, P.A. Amendt, et al., Charged-particle probing of x-ray-driven inertial-fusion implosions, Science 327 (2010) 1231–1235.
[25] C.K. Li, F.H. Séguin, J.A. Frenje, M.J. Rosenberg, H.G. Rinerknecht, A.B. Zylstra, et al., Impeding hohlraum plasma stagnation in inertial-confinement fusion, Phys. Rev. Lett. 108 (2012) 025001.
[26] A.B. Zylstra, J.A. Frenje, P.E. Grabowski, C.K. Li, G.W. Collins, P. Fitzsimmons, et al., Measurement of charged-particle stopping in warm dense plasma, Phys. Rev. Lett. 114 (2015) 215002, doi:10.1103/PhysRevLett.114.215002.
[27] G.H. Miller, E.I. Moses, C.R. Wuest, The national ignition facility, Opt. Eng. 43 (12) (2004) 2841–2853, doi:10.1117/1.1814767.
[28] M.J. Rosenberg, A.B. Zylstra, F.H. Séguin, H.G. Rinderknecht, J.A. Frenje, M. Gatu Johnson, et al., Investigation of ion kinetic effects in direct-drive exploding-pusher implosions at the NIF, Phys. Plasmas 21 (12) (2014) 122712.
[29] S. Skupsky, J.A. Marozas, R.S. Craxton, R. Betti, T.J.B. Collins, J.A. Delettrez, et al., Polar direct drive on the National Ignition Facility, Phys. Plasmas 11 (2004) 2763–2770, doi:10.1063/1.1689665.
[30] V.Y. Glebov, C. Stoeckl, T.C. Sangster, S. Roberts, G.J. Schmid, R.A. Lerche, et al., Prototypes of national ignition facility neutron time-of-flight detectors tested on omega, Rev. Sci. Instrum. 75 (10) (2004) 3559–3562.
[31] F.H. Séguin, J.A. Frenje, C.K. Li, D.G. Hicks, S. Kurebayashi, J.R. Rygg, et al., Spectrometry of charged particles from inertial-confinement-fusion plasmas, Rev. Sci. Instrum. 74 (2) (2003) 975–995.
[32] F.H. Séguin, N. Sinenian, M. Rosenberg, A. Zylstra, M.J.-E. Manuel, H. Sio, et al., Advances in compact proton spectrometers for inertial-confinement fusion and plasma nuclear science, Rev. Sci. Instrum. 83 (10) (2012) 10D908.
[33] A.B. Zylstra, J.A. Frenje, F.H. Séguin, M.J. Rosenberg, H.G. Rinderknecht, M.G. Johnson, et al., Charged-particle spectroscopy for diagnosing shock R and strength in NIF implosions, Rev. Sci. Instrum. 83 (10) (2012) 10D901.
[34] H.G. Rinderknecht, M.G. Johnson, A.B. Zylstra, N. Sinenian, M.J. Rosenberg, J.A. Frenje, et al., A novel particle time of flight diagnostic for measurements of shock- and compression-bang times in D^3He and DT implosions at the NIF, Rev. Sci. Instrum. 83 (2012) 10D902.
[35] R.L. Fleischer, P.B. Price, R.M. Walker, Ion explosion spike mechanism for formation of charged-particle tracks in solids, J. Appl. Phys. 36 (1965) 3645.
[36] G. Dajkó, Proton detection with CR-39 track detector, Radiat. Prot. Dosimetry 66 (1–4) (1996) 359–362.
[37] H.G. Rinderknecht, M.J. Rosenberg, C.K. Li, N.M. Hoffman, G. Kagan, A.B. Zylstra, et al., Ion thermal decoupling and species separation in shock-driven implosions, Phys. Rev. Lett. 114 (2015) 025001, doi:10.1103/PhysRevLett.114.025001 <http://link.aps.org/doi/10.1103/PhysRevLett.114.025001>.
[38] C.K. Li, D.G. Hicks, F.H. Séguin, J.A. Frenje, R.D. Petrasso, J.M. Soures, et al., D-^{3}He proton spectra for diagnosing shell ρR and fuel T_i of imploded capsules at OMEGA, Phys. Plasmas 7 (6) (2000) 2578–2584.
[39] D.H. Edgell, D.K. Bradley, E.J. Bond, S. Burns, D.A. Callahan, J. Celeste, et al., South pole bang-time diagnostic on the national ignition facility (invited), Rev. Sci. Instrum. 83 (2012) 10E119.
[40] S. Glenn, J. Koch, D.K. Bradley, N. Izumi, P. Bell, G. Stone, et al., A hardened gated x-ray imaging diagnostic for inertial confinement fusion experiments at the national ignition facility, Rev. Sci. Instrum. 81 (2010) 10E539.
[41] G.A. Kyrala, S. Dixit, S. Glenzer, D. Kalantar, D. Bradley, N. Izumi, et al., Measuring symmetry of implosions in cryogenic *Hohlraums* at the NIF using gated x-ray detectors (invited), Rev. Sci. Instrum. 81 (2010) 10E316.
[42] M.J. Rosenberg, A.B. Zylstra, J.A. Frenje, H.G. Rinderknecht, M. Gatu Johnson, C.J. Waugh, et al., A compact proton spectrometer for measurement of the absolute DD proton spectrum from which yield and R are determined in thin-shell inertial-confinement-fusion implosions, Rev. Sci. Instrum. 85 (10) (2014) 103504.
[43] M.J. Rosenberg, F.H. Séguin, C.J. Waugh, H.G. Rinderknecht, D. Orozco, J.A. Frenje, et al., Empirical assessment of the detection efficiency of CR-39 at high proton fluence and a compact, proton detector for high-fluence applications, Rev. Sci. Instrum. 85 (4) (2014) 043302.
[44] H. Sio, F.H. Sguin, J.A. Frenje, M. Gatu Johnson, A.B. Zylstra, H.G. Rinderknecht, et al., A technique for extending by ~10^3 the dynamic range of compact proton spectrometers for diagnosing ICF implosions on the national ignition facility and OMEGA, Rev. Sci. Instrum. 85 (11) (2014) 11E119.
[45] C.J. Waugh, M.J. Rosenberg, A.B. Zylstra, J.A. Frenje, F.H. Séguin, R.D. Petrasso, et al., A method for in situ absolute DD yield calibration of neutron time-of-flight detectors on OMEGA using CR-39-based proton detectors, Rev. Sci. Instrum. 86 (5) (2015) 053506.
[46] M.J. Rosenberg, H.G. Rinderknecht, N.M. Hoffman, P.A. Amendt, S. Atzeni, A.B. Zylstra, et al., Exploration of the transition from the hydrodynamiclike to the strongly kinetic regime in shock-driven implosions, Phys. Rev. Lett. 112 (2014) 185001, doi:10.1103/PhysRevLett.112.185001.
[47] S.F. Khan, P.M. Bell, D.K. Bradley, S.R. Burns, J.R. Celeste, L.S. Dauffy, et al., Measuring x-ray burn history with the streaked polar instrumentation for diagnosing energetic radiation (SPIDER) at the National Ignition Facility (NIF), Proc. SPIE (2012). doi:10.1117/12.930032.
[48] C. Stoeckl, V.Y. Glebov, S. Roberts, T.C. Sangster, R.A. Lerche, R.L. Griffith, et al., Ten-inch manipulator-based neutron temporal diagnostic for cryogenic experiments on OMEGA, Rev. Sci. Instrum. 74 (3) (2003) 1713–1716.
[49] F.H. Séguin, J.L. Deciantis, J.A. Frenje, S. Kurebayashi, C.K. Li, C. Chen, et al., D^3He-proton emission imaging for inertial-confinement-fusion experiments (invited), Rev. Sci. Instrum. 75 (10) (2004) 3520–3525.
[50] J.R. Rygg, J.A. Frenje, C.K. Li, F.H. Séguin, R.D. Petrasso, F.J. Marshall, et al., Observations of the collapse of asymmetrically driven convergent shocks, Phys. Plasmas 15 (2008) 034505.
[51] O.A. Hurricane, private communication (2014).
[52] S. Le Pape, L. Divol, L. Berzak Hopkins, A. Mackinnon, N. Meezan, D. Casey, et al., Observation of a reflected shock in an indirectly driven spherical implosion at the national ignition facility, Phys. Rev. Lett. 112 (2014) 225002, doi:10.1103/PhysRevLett.112.225002.
[53] A.B. Zylstra, J.A. Frenje, F.H. Séguin, D.G. Hicks, E.L. Dewald, H.F. Robey, et al., The effect of shock dynamics on compressibility of ignition-scale national ignition facility implosions, Phys. Plasmas 21 (11) (2014) 112701.
[54] M.J. Rosenberg, F.H. Séguin, P.A. Amendt, S. Atzeni, H.G. Rinderknecht, N.M. Hoffman, et al., Assessment of ion kinetic effects in shock-driven inertial confinement fusion implosions using fusion burn imaging, Phys. Plasmas 22 (6) (2015) 062702.
[55] J.L. DeCiantis, F.H. Séguin, J.A. Frenje, V. Berube, M.J. Canavan, C.D. Chen, et al., Proton core imaging of the nuclear burn in inertial confinement fusion implosions, Rev. Sci. Instrum. 77 (2006) 043503.
[56] F.H. Séguin, J.L. DeCiantis, J.A. Frenje, C.K. Li, J.R. Rygg, C.D. Chen, et al., Measured dependence of nuclear burn region size on implosion parameters in inertial confinement fusion experiments, Phys. Plasmas 13 (2006) 082704.
[57] D.K. Bradley, P.M. Bell, O.L. Landen, J.D. Kilkenny, J. Oertel, Development and characterization of a pair of 30-40 ps x-ray framing cameras, Rev. Sci. Instrum. 66 (1) (1995) 716–718.